Supporting Information

# A Turn-On AIE Sensor for Nanomolar Detection of Perrhenate in Aqueous Media

Yan-ni Li, Yan-xin Du, Hao Liu, Yi-jie Zhu, Fan Deng, Qin-feng Xu*

School of Food Science and Engineering, National Research and Development Center for Goat Dairy Products Processing Technology, Shaanxi University of Science and Technology, Xi'an, Shaanxi 710021, China.

* Corresponding Authors. Email: xuqinfeng@sust.edu.cn.

## 1. Supplementary Figures

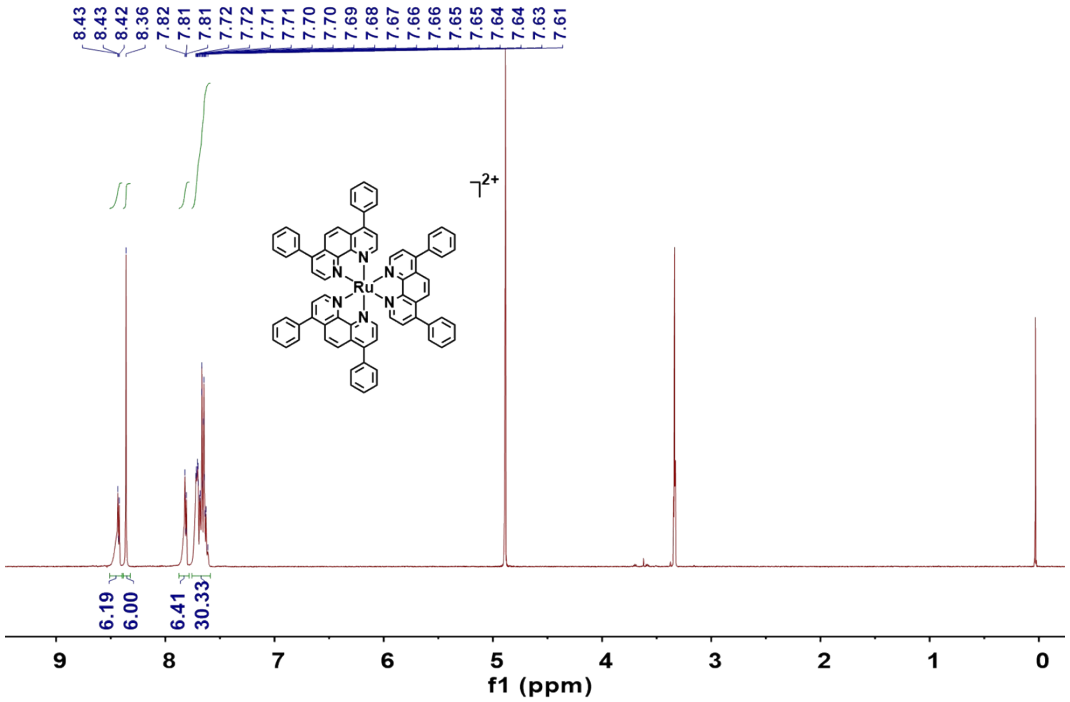


**Fig. S1** $^{1}$H NMR spectrum of probe **Ru1** in $CD_4O$.

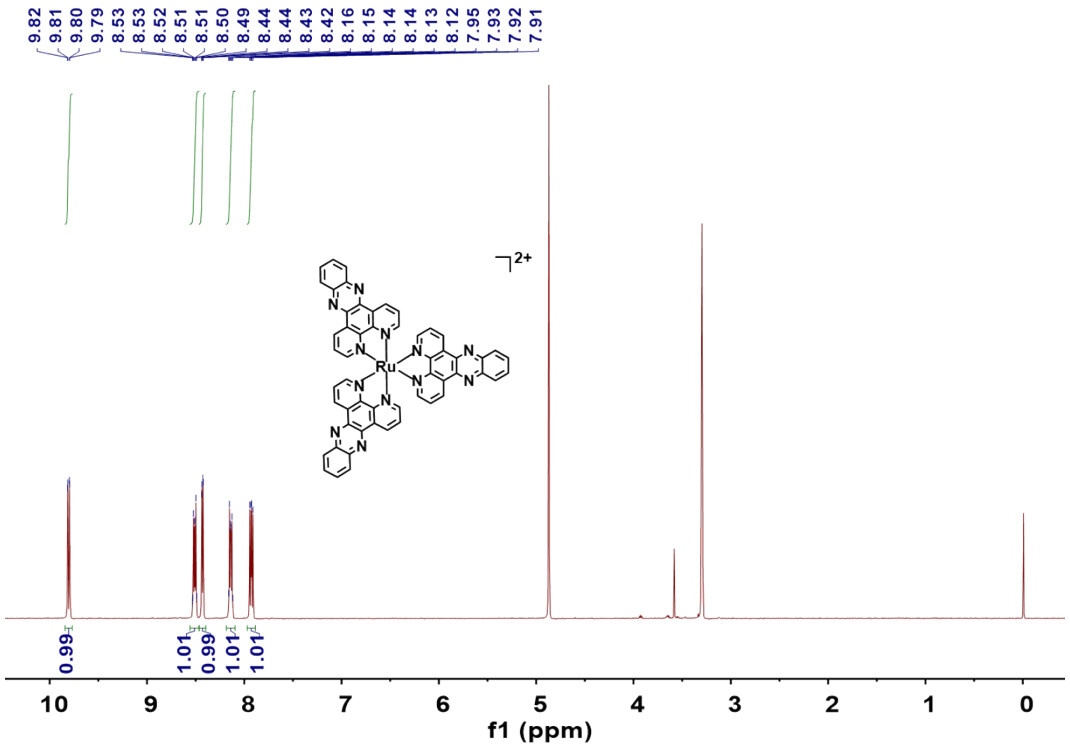


**Fig. S2** $^{1}$H NMR spectrum of probe **Ru2** in $CD_4O$.

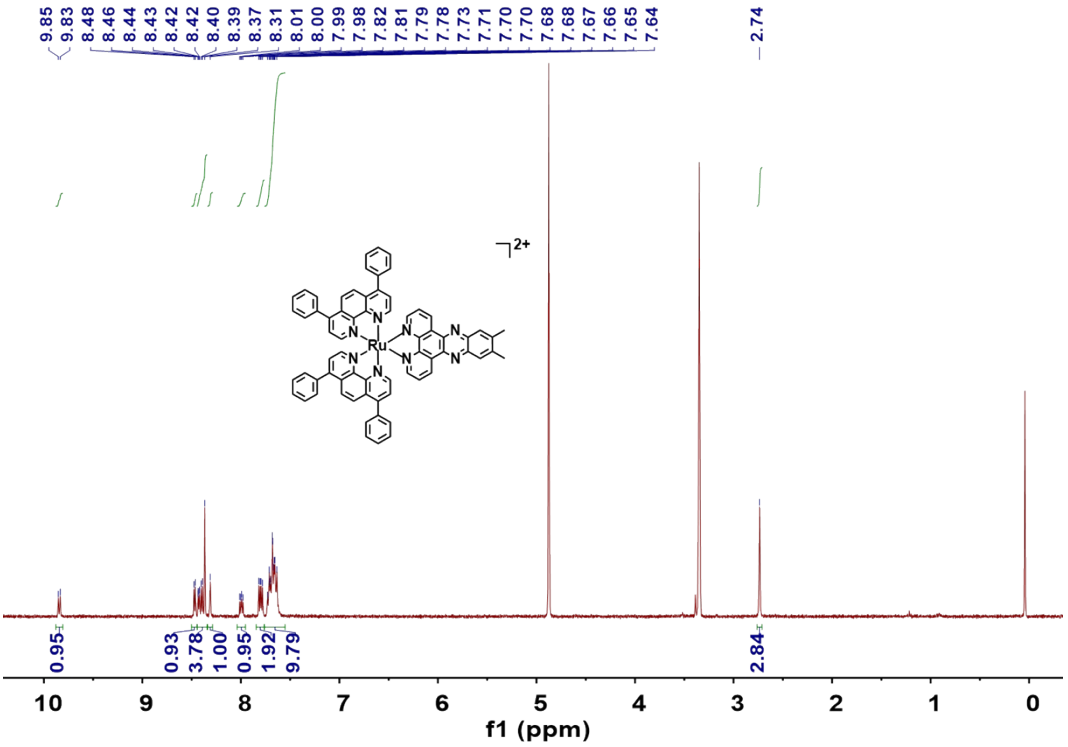


**Fig. S3** $^{1}$H NMR spectrum of probe **Ru3** in $CD_4O$.

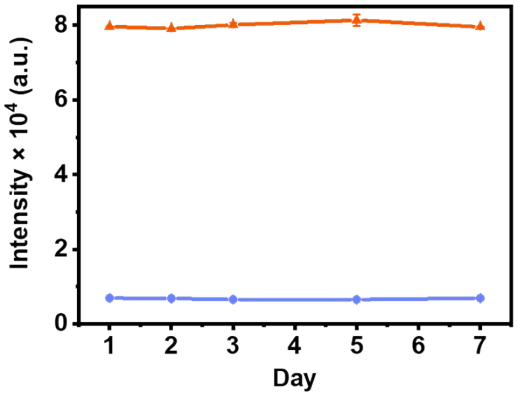


**Fig. S4** Stability test of **Ru3** aqueous solution at room temperature over 7 days in the absence and presence of $ReO_4^-$.

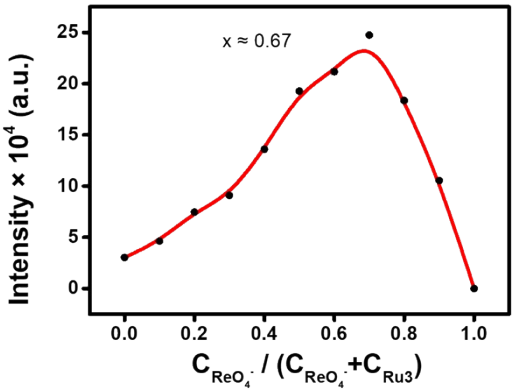


**Fig. S5** Job plot of Luminescence intensity of **Ru3** with $ReO_4^-$ in water (total concentration: 50 μM).

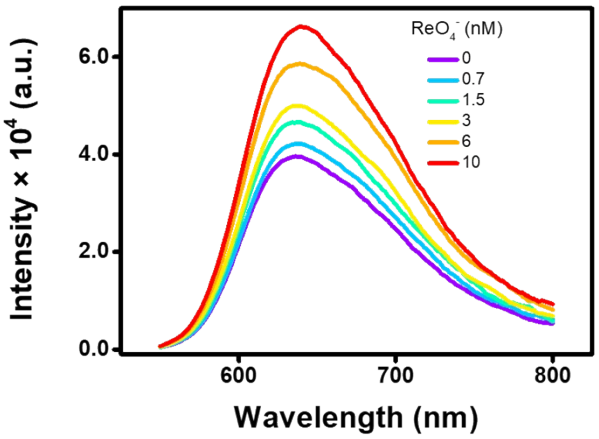


**Fig. S6** Luminescence emission spectra of **Ru3** in the presence of different concentrations of $ReO_4^-$ with preconcentration.

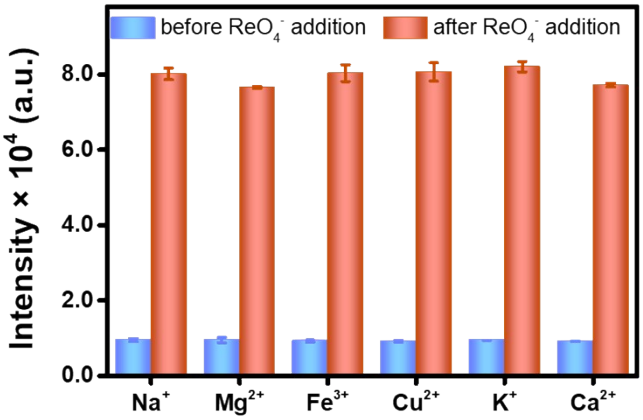


**Fig. S7** Luminescence responses of probe **Ru3** in the presence of different cationic analytes.

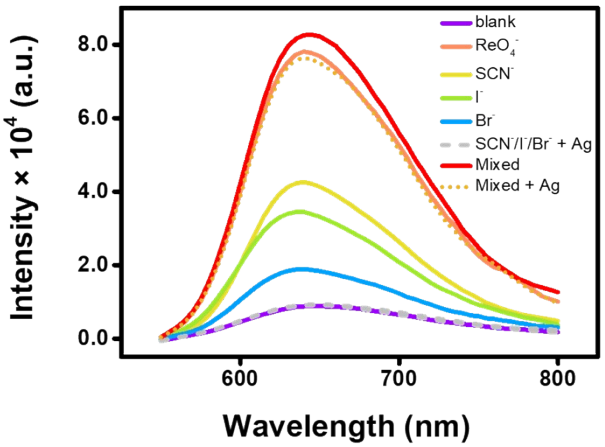


**Fig. S8** Luminescence emission spectra of **Ru3** to $ReO_4^-$ and other anions without and with treatment of IC-Ag column.

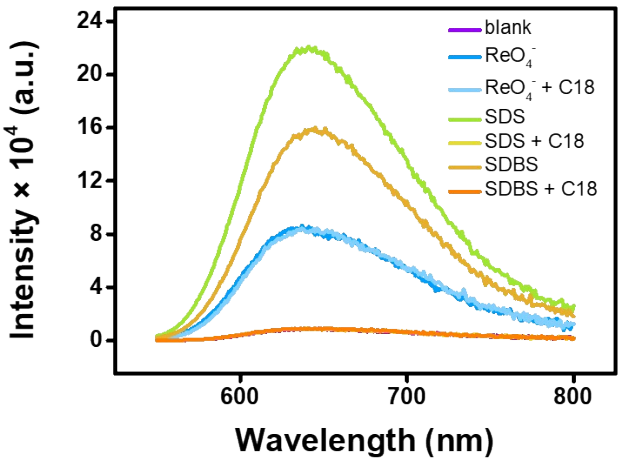


**Fig. S9** Luminescence responses of **Ru3** (20 μM) toward $ReO_4^-$ and other organic compounds (10 μM) without and with treatment of C18 column.

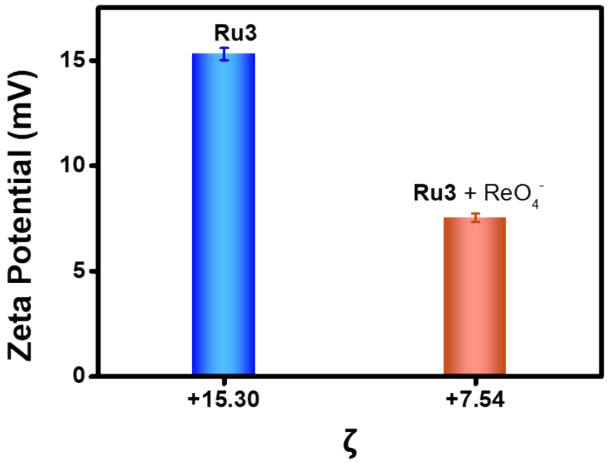


**Fig. S10** Comparative Zeta potential study of **Ru3** in the absence and presence of $ReO_4^-$.

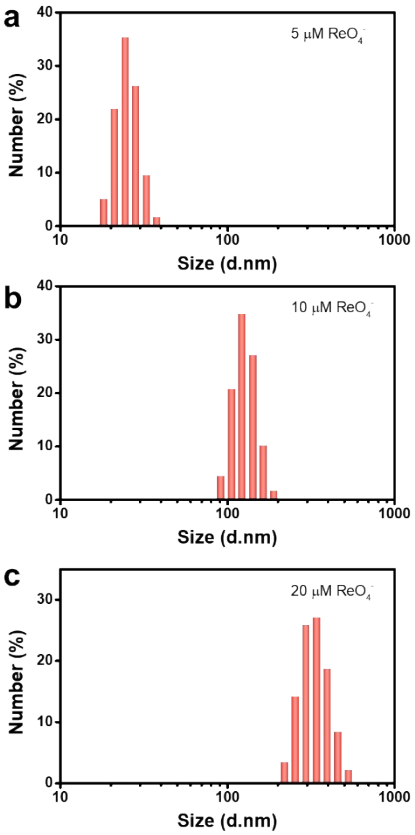


**Fig. S11** DLS profiles of **Ru3** in the presence of different concentrations of $ReO_4^-$. (a) 5 μM，(b) 10 μM, (c) 20 μM.

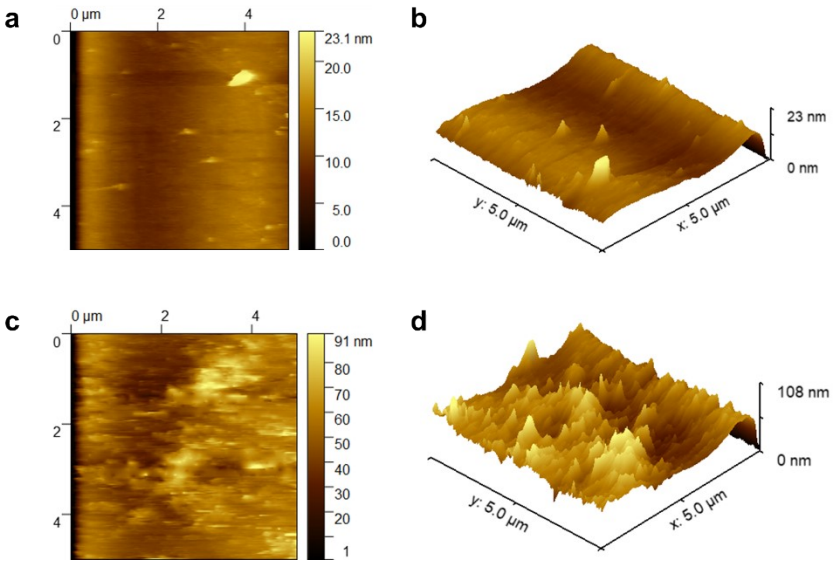


**Fig. S12** AFM images of **Ru3** in the absence and presence of $ReO_4^-$. (a) 2D and (b) 3D image without $ReO_4^-$, (c) 2D and (d) 3D image with $ReO_4^-$.

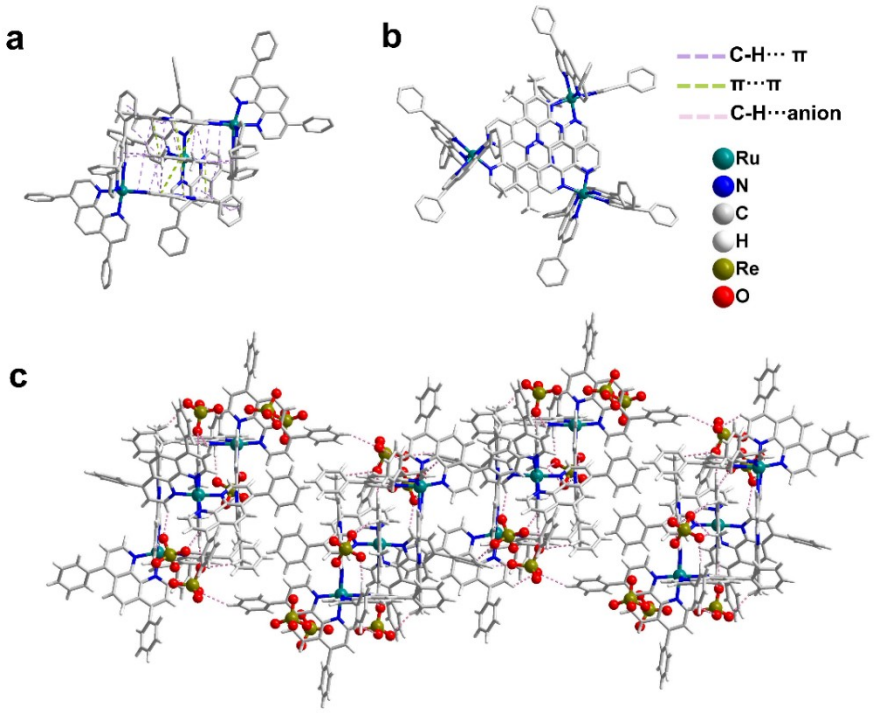


**Fig. S13** (a) Side view and (b) top view of the crystal structure of [**Ru3**]$(ReO_4)_2$ adduct complexes. Solvent molecules and hydrogen atoms are omitted for clarity. The purple and the green dotted line represent the C-H··· π interaction and the π···π interaction in the adjacent molecules of **Ru3**, respectively; (c) View of the three-dimensional (3D) crystal packing of [**Ru3**]$(ReO_4)_2$ adduct complexes.

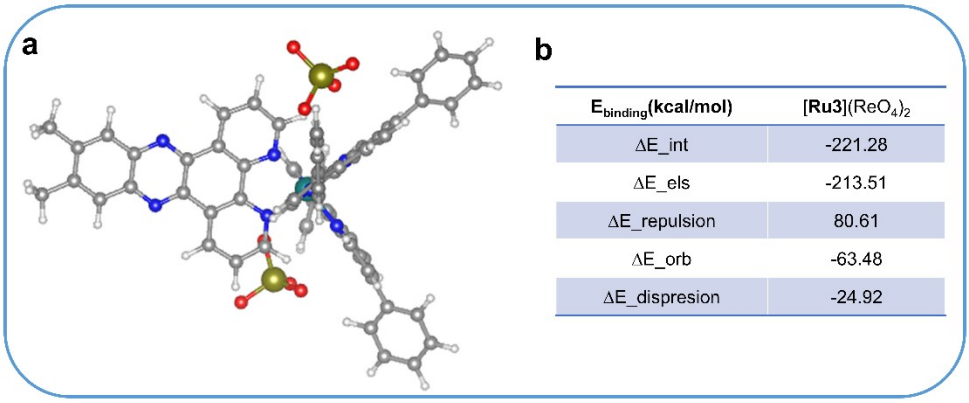


| $E_{binding}$(kcal/mol) | [Ru3]$(ReO_4)_2$ |
|---|---|
| ΔE_int | -221.28 |
| ΔE_els | -213.51 |
| ΔE_repulsion | 80.61 |
| ΔE_orb | -63.48 |
| ΔE_dispresion | -24.92 |

**Fig. S14** (a) The optimized structure of the [**Ru3**]$(ReO_4)_2$ complex. (b) Energy decomposition analysis of the [**Ru3**]$(ReO_4)_2$ complex.

## 2. Supplementary Tables

**Table S1.** Sensitivity comparation of the present probe with the recently reported luminescence probes for $ReO_4^-$.

| Detection manner | Materials | Detection mechanism | Solvent | Response time | LOD (μM) | Ref. |
|---|---|---|---|---|---|---|
| turn-off | CP-16 | aggregation-induced fluorescence quenching | water and a chloroform/methanol (1:1) mixture | - | 0.58 | [1] |
| turn-off | TJNU-302 | electron transfer | $H_2O$ | - | 90 | [2] |
| turn-off | $Zr^{4+}$ MOFs | electron transfer | $H_2O$ | | 0.55 | [3] |
| turn-off | NCU-2 | ion exchange | $H_2O$ | ＜30 s | 0.067 | [4] |
| turn-off | PMA | Photoinduced electron transfer (PET) | $H_2O$ | - | 14 | [5] |
| turn-off | MOCNs | PET | $H_2O$ | - | 12.6 | [6] |
| turn-off | BTTA–BDNP | PET | DMF/$H_2O$ | ＜30 s | 0.067 | [7] |
| turn-off | TFPM-EP-Br | PET | $H_2O$ | ＜2 s | 0.033 | [8] |
| turn-off | TpBDOH-AB | ion exchange | $C_2H_5OH$ | 2 s | 1.07 | [9] |
| turn-off | C-CD | PET | $H_2O$ | - | 87 | [10] |
| turn-off | $1H_6^{6+}$ | PET | 0.1 M $CF_3SO_3Na$, pH = 2 | - | - | [11] |
| turn-off | ModA | hydrogen bond | 20 mM Tris, 50 mM NaCl, pH = 7.6 | - | - | [12] |
| turn-on | TPDC-I | AIE | $H_2O$ | - | 0.9 | [13] |
| turn-on | XB | halogen bonding and electrostatic interaction | 10 mM aqueous hepes buffer, pH = 7.4 | - | - | [14] |
| turn-on | PIC | J-aggregation | $H_2O$ | - | 0.17 | [15] |
| turn-on | ThT | AIE | $H_2O$ | - | 260 | [16] |
| turn-on | AuO | J-aggregation | $H_2O$ | - | 270 | [17] |

**Table S1**: (continued)

| Detection manner | Materials | Detection mechanism | Solvent | Response time | LOD (μM) | Ref. |
|---|---|---|---|---|---|---|
| turn-on | [Pt(tpy)Br](SbF$_6$) | ion exchange | $H_2O$ | 2-5 min | $2.6 \times 10^{-4}$ | [18] |
| turn-on | Ir-PAF | ion exchange | pH = 4 | - | 2.07 | [19] |
| turn-on | Ru(II) complex | halogen-bond | acetonitrile | - | - | [20] |
| turn-on | **Ru1** | AIE | $H_2O$ | ＜1 s | 0.718 | this work |
| turn-on | **Ru2** | AIE | $H_2O$ | ＜1 s | 0.026 | |
| turn-on | **Ru3** | AIE | $H_2O$ | ＜1 s | 0.003 | |
| turn-on | **Ru3** | AIE | $H_2O$ | ＜1 s | $1.3 \times 10^{-4}$ (after pre-concentration) | |

**Table S2.** Composition of simulated Hanford LAW melter recycle stream.

| Anion | Concentration(mol/L) | Anion: $TcO_4^-$ molar ratio |
|---|---|---|
| $TcO_4^-$ | $1.94 \times 10^{-4}$ | 1.0 |
| $NO_3^-$ | $6.07 \times 10^{-2}$ | 314 |
| $Cl^-$ | $6.39 \times 10^{-2}$ | 330 |
| $NO_2^-$ | $1.69 \times 10^{-1}$ | 873 |
| $SO_4^{2-}$ | $6.64 \times 10^{-6}$ | 0.0343 |
| $CO_3^{2-}$ | $4.30 \times 10^{-5}$ | 0.222 |

**Table S3.** Summary of X-Ray Crystallographic Data.

| **Complexes** | [**Ru3**]$(ReO_4)_2$ |
|---|---|
| **Empirical formula** | $C_{204}H_{138}N_{24}O_{24}Re_6Ru_3$ |
| **Formula weight** | 4729.79 |
| **Temperature/K** | 193.00 |
| **Crystal system** | monoclinic |
| **Space group** | $P2_1/c$ |
| **Unit cell dimensions** | a = 31.456(17) Å, α = 90°<br>b = 24.499(13) Å, β = 106.554(9)°<br>c = 29.263(16) Å, γ = 90° |
| **Volume/Å$^3$** | 21616(20) |
| **Z** | 4 |
| **$\rho_{calc}$g/cm$_3$** | 1.453 |
| **μ/mm$^{-1}$** | 3.612 |
| **F(000)** | 9216.0 |
| **Crystal size/mm$^3$** | 0.12 × 0.1 × 0.09 |
| **Radiation** | MoKα (λ = 0.71073) |
| **2Θ range for data collection/°** | 3.906 to 49.424 |
| **Index ranges** | -37≤ h ≤ 37, -28 ≤ k ≤ 28, -34≤ l ≤ 34 |
| **Goodness-of-fit on F$^2$** | 1.230 |
| **Final R indexes [I>=2σ (I)]** | $R_1$ = 0.1494, $wR_2$ = 0.3459 |
| **Final R indexes [all data]** | $R_1$ = 0.1774, $wR_2$ = 0.3604 |
| **Largest diff. peak/hole /eÅ$^{-3}$** | 1.76/-1.71 |

## 3. References


1. A. Hazra, C. Ghosh, F. Banerjee and S. K. Samanta, Highly efficient main-chain cationic polyelectrolytes for selective sensing of permanganate, perrhenate, and heparin. *ACS Appl. Polym. Mater.*, 2024, **6**, 6540-6551.
2. C.-P. Li, H. Zhou, J. Chen, J.-J. Wang, M. Du and W. Zhou, A highly efficient coordination polymer for selective trapping and sensing of perrhenate/pertechnetate. *ACS Appl. Mater. Interfaces*, 2020, **12**, 15246-15254.
3. S. Rapti, S. A. Diamantis, A. Dafnomili, A. Pournara, E. Skliri, G. S. Armatas, A. C. Tsipis, I. Spanopoulos, C. D. Malliakas and M. G. Kanatzidis, Exceptional $TcO_4^-$ sorption capacity and highly efficient $ReO_4^-$ luminescence sensing by $Zr^{4+}$ MOFs. *J. Mater. Chem. A*, 2018, **6**, 20813-20821.
4. Q.-H. Hu, X. Gao, Y.-Z. Shi, R.-P. Liang, L. Zhang, S. Lin and J.-D. Qiu, Tailor-made multiple interpenetrated metal-organic framework for selective detection and adsorption of $ReO_4^-$. *Anal. Chem.*, 2022, **94**, 16864-16870.
5. G. Singh, S. P. Pandey and P. K. Singh, A dual intensity and lifetime based fluorescence sensor for perrhenate anion. *Sens. Actuators, B*, 2021, **330**, 129346.
6. S. Khan and S. K. Mandal, Luminescent 2D pillared-bilayer metal-organic coordination networks for selective sensing of $ReO_4^-$ in water. *ACS Appl. Mater. Interfaces*, 2021, **13**, 45465-45474.
7. X.-R. Chen, C.-R. Zhang, X. Liu, R.-P. Liang and J.-D. Qiu, Ionic covalent organic framework for selective detection and adsorption of $TcO_4^-$/$ReO_4^-$. *Chem. Commun.*, 2023, **59**, 9521-9524.
8. J.-X. Qi, C.-R. Zhang, X.-J. Chen, S.-M. Yi, C.-P. Niu, J.-L. Liu, L. Zhang, R.-P. Liang and J.-D. Qiu, 3D ionic olefin-linked conjugated microporous polymers for selective detection and removal of $TcO_4^-$/$ReO_4^-$ from wastewater. *Anal. Chem.*, 2022, **94**, 10850-10856.
9. S.-M. Yi, C.-R. Zhang, W. Jiang, X. Liu, C.-P. Niu, J.-X. Qi, X.-J. Chen, R.-P. Liang and J.-D. Qiu, Ionic liquid modified covalent organic frameworks for efficient detection and adsorption of $ReO_4^-$/$TcO_4^-$. *J. Environ. Chem. Eng.*, 2022, **10**, 107666.
10. M. R. Choi and B. Lee, Synthesis of cationic carbon quantum dot-based dual emission fluorescence sensor for detecting perrhenate anions in aqueous solutions. *Opt. Mater.*, 2022, **134**, 113190.
11. V. Amendola, G. Bergamaschi, M. Boiocchi, R. Alberto and H. Braband, Fluorescent sensing of $^{99}Tc$ pertechnetate in water. *Chem. Sci.*, 2014, **5**, 1820-1826.
12. B. P. Aryal, P. Brugarolas and C. He, Binding of $ReO_4^-$ with an engineered $MoO_4^{2-}$-binding protein: towards a new approach in radiopharmaceutical applications. *JBIC, J. Biol. Inorg. Chem.*, 2012, **17**, 97-106.
13. H.-L. Xu, J.-Y. Zhang, J.-S. Su, L. Li, H.-Y. Cao, G.-L. Li and Z.-H. Ni, Efficient capture and dual-model fluorescence detection of $ReO_4^-$ using a TPE-based pyridinium network. *Dyes Pigm.*, 2025, **235**, 112579.
14. J. Y. Lim and P. D. Beer, Superior perrhenate anion recognition in water by a halogen bonding acyclic receptor. *Chem. Commun.*, 2015, **51**, 3686-3688.
15. S. P. Pandey, A. M. Desai and P. K. Singh, A highly sensitive fluorescence “turn on” detection of perrhenate Anion, a non-radioactive surrogate of hazardous pertechnetate anion. *Sens. Actuators, B*, 2020, **323**, 128675.

16. A. M. Desai and P. K. Singh, An ultrafast molecular-rotor-based fluorescent turn-on sensor for the perrhenate anion in aqueous solution. *Chem. - Eur. J.*, 2019, **25**, 2035-2042.
17. A. M. Desai and P. K. Singh, Ratiometric fluorescence turn-on sensing of perrhenate anion, a non-radioactive surrogate of hazardous pertechnetate, in aqueous solution. *Sens. Actuators, B*, 2018, **277**, 205-209.
18. S. Chatterjee, A. E. Norton, M. K. Edwards, J. M. Peterson, S. D. Taylor, S. A. Bryan, A. Andersen, N. Govind, T. E. Albrecht-Schmitt and W. B. Connick, Highly selective colorimetric and luminescence response of a square-planar platinum(II) terpyridyl complex to aqueous $TcO_4^-$. *Inorg. Chem.*, 2015, **54**, 9914-9923.
19. D.-Y. Xu, L. Chen, X. Dai, B.-Y. Li, Y.-X. Wang, W. Liu, J. Li, Y. Tao, Y.-L. Wang, Y. Liu, G.-W. Peng, R.-H. Zhou, Z.-F. Chai, S.-A. Wang, A porous aromatic framework functionalized with luminescent iridium(III) organometallic complexes for turn-on sensing of $^{99}TcO_4^-$. *ACS Appl. Mater. Interfaces*, 2020, **12**, 15288-15297.
20. S. Mondal, A. Rashid and P. Ghosh, A pentafluorophenyl functionalized RuII-probe having halogen bond center toward recognition and sensing of perrhenate and dihydrogen phosphate. *J. Organomet. Chem.*, 2021, **952**, 122027.